

T-scanner for measuring pulse durations

A. DREISCHUH, I. BUCHVAROV, E. EUGENIEVA, S. DINEV
Department of Physics, Sofia University, 5 J. Bourchier Blvd., BG-1164 Sofia, Bulgaria

V. MARINOV
Institute of Electronics, Bulgarian Academy of Sciences, 72 Tzarigradsko Shosse Blvd., BG-1784 Sofia, Bulgaria

Received 9 August 1995; revised 17 February; accepted 22 March 1996

A method for ultrashort pulse-duration measurement is analysed both theoretically and experimentally. The approach is based on a time-resolved induced phase modulation of a probe beam-pulse in a two-colour Z-scan configuration. The experimental results presented are in good agreement with the simple analytical result derived for retrieving unknown pulse width.

1. Introduction

In recent years there has been significant progress in the generation of short and ultrashort light pulses in the infrared to ultraviolet (u.v.) spectral range [1–3]. Development of novel approaches for pulse-duration measurement accompanied these efforts. Presently, streak-cameras allow pulse widths down to several hundreds of femtoseconds to be measured in a broad spectral range. Most frequently, single- and multiple-shot correlation techniques are employed [4]. Since there are no non-linear crystals simultaneously able to be phase matched below 400 nm and transparent below 197 nm [5], alternative non-linear effects, such as two-photon fluorescence [6] and multiphoton ionization [7], are used to measure pulse durations. It has been demonstrated that two-photon absorption in diamond is strong enough to permit measurements of ultraviolet and visible (220–550 nm) pulse widths [8]. Ultraviolet and visible pulses could be measured also by detecting the light-excited acoustic wave [9, 10].

The 'Z-scan' technique can be used for a sensitive measurement of non-linear refraction and absorption of various materials [11]. It consists of using a single tight-focused Gaussian beam and measuring the transmittance of a non-linear medium through a finite aperture in the far field as a function of sample position, z , measured with respect to the focal plane. Using a material with positive non-linearity and thickness smaller than the diffraction length, z_0 , of the focused beam, a prefocal transmittance minimum and a post-focal transmittance maximum has been obtained [11]. Recently, the Z-scan technique has been modified for measuring non-degenerate non-linear refractive indices, $n_2(\omega_p, \omega_c)$, and non-degenerate two-photon absorption coefficients, $\beta_2(\omega_p, \omega_c)$ [12–14], with a temporal resolution in the picosecond time-scale [15].

In this paper the authors analyse theoretically and experimentally a method for laser pulse-width measurement, based on Z-scan geometry with variable temporal delay (namely a

'T-scanner'). The technique is based on induced-phase modulation on a probe beam-pulse by a pump and seems reliable and simple. The problem was treated both numerically (by the split-step Fourier method) and variationally. Three non-linear media were considered: BaF₂ crystal with an electronic non-linearity, CS₂ with reorientational Kerr non-linearity and Xe gas under quasi-resonant conditions. The experimental results presented are in good agreement with the simple analytical relation derived.

2. Numerical analysis

The arrangement analysed is depicted in Fig. 1. Inside the non-linear medium the two copropagating pulses at different wavelengths, λ_s and λ_p , are coupled through cross-phase modulation (XPM). In a pump-probe beam-pulse configuration the XPM reduces to pump-induced phase modulation (IPM) [16]. The beams are focused with an achromatic lens of focal length, f ; z_0 is the diffraction length of the probe beam and L_0 is the distance between the waist of the probe and the aperture. The non-linear medium of thickness, L , is considered to be self-focusing and is placed at $z = 0.86z_0$. This value of z corresponds to the maximum aperture transmittance of the probe [11]. A photodetector transducer placed behind the aperture, A, measures the signal energy, integrated in time (over time profile of probe pulse) and in space (over the aperture cross-section). Due to the IPM, acting on the probe and originating in the strong pump beam-pulse, the non-linear medium plays the role of a thin focusing lens (at $z > 0$), which collimates the probe beam leading to an increase in the energy transmitted through the aperture. The filter, F, transmits only the probe wave. Stronger pump intensities result in stronger beam focusing and larger aperture transmittances. It should be noted that at $n_2 < 0$ or at $z < 0$ the probe beam-pulse behaviour reverses. In the presence of a temporal delay, τ_d , between the pulses, the energy transmitted is found to be smaller than the energy transmitted in the absence of a temporal delay [12]. One can expect that this decrease depends simultaneously on the temporal delay, τ_d , between the pulses, and on the pump- and probe-pulse durations, τ_p and τ_s , respectively. In the following the authors will show that this dependence provides an opportunity to estimate laser pulse durations. Gaussian beams-pulses are assumed. Generally, the beam-pulse propagation in the T-scanner is

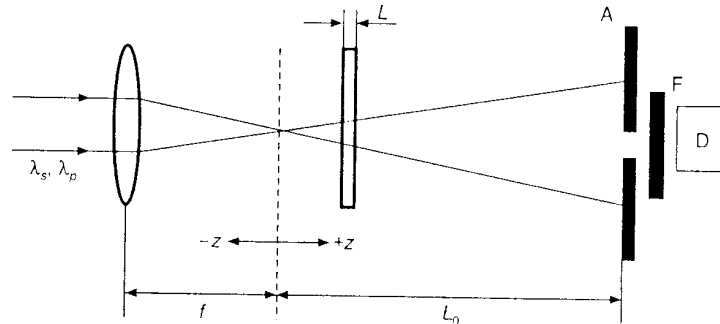


Figure 1 Proposed experimental scheme (λ_s , λ_p , wavelengths of the incoming pulses; f , lens focal length; z , position of the non-linear medium of thickness, L , measured from the linear beam waist; L_0 , linear beam waist-to-aperture distance; A, aperture; F, filter; D, detector transducer).

described by two coupled-amplitude non-linear Schrödinger equations [17, 18]:

$$i \left(\frac{\partial}{\partial z} + \frac{1}{V_{g_j}} \frac{\partial}{\partial t} \right) \psi_j + \frac{1}{2} \beta_{2j} \frac{\partial^2 \psi_j}{\partial t^2} + \alpha_j \left(\frac{\partial^2 \psi_j}{\partial x^2} + \frac{\partial^2 \psi_j}{\partial y^2} \right) + k^{\text{SPM}}(\lambda_j) |\psi_j|^2 \psi_j + k^{\text{XPM}}(\lambda_j) |\psi_l|^2 \psi_j = 0 \quad (1)$$

where $j, l = s, p; j \neq l$;

$$k^{\text{SPM}}(\lambda_j) = \frac{n_2^{\text{SPM}}(\lambda_j) k_j}{2n_0} \quad (2a)$$

$$k^{\text{XPM}}(\lambda_j) = \frac{n_2^{\text{XPM}}(\lambda_j) k_j}{2n_0} \quad (2b)$$

$$\beta_{2s,p} = \frac{\lambda_{s,p}^3}{2\pi c^2} \left(\frac{\partial^2 n}{\partial \lambda^2} \right)_{\lambda=\lambda_{s,p}} \quad (2c)$$

$$\alpha_{s,p} = -1/(2k_{s,p}) \quad (2d)$$

ψ_p and ψ_s are the amplitudes of the pump and probe waves, V_{g_p} and V_{g_s} are their group velocities, $k_{s,p}$ are the respective wave numbers, $\alpha_{s,p}$ account for the beam diffraction, $\beta_{2s,p}$ are the corresponding group-velocity dispersion coefficients, k^{SPM} and k^{XPM} account for the self-phase modulation and cross-phase modulation, n_2^{SPM} and n_2^{XPM} are the corresponding non-linear refraction indices, whereas n_0 are the corresponding linear ones. Owing to the limited computing resources available, the authors solved Equation 1 using a modification of the split-step Fourier method under the following conditions:

(a) The pump intensity is assumed much higher than the probe intensity (pump-probe regime). As a result, the influence of the probe on the pump and the self-action of the probe can be neglected, i.e. the only non-linear effect on the probe wave is the IPM from the pump.

(b) Since the arrangement is axially symmetric, the transverse beam-pulse evolution is expected to be symmetric too.

(c) The thickness, L , of the non-linear medium is chosen to be much smaller than z_0 , i.e. the non-linear lens formed is a thin one. In this case the pulse walk-off length $L_W = \tau_{\text{HW1-ej}}/|v_{s,p}|$ is much larger than L , where $v_{s,p} = (V_{g_s}^{-1} - V_{g_p}^{-1})$ is the group-velocity mismatch. This enables one to claim that the initial delay, τ_d , between the pulses remains nearly unchanged during the pulse propagation inside the non-linear medium.

(d) The dispersive length, $L_D = \tau_{\text{HW1-ej}}^2/|\beta_{2s,p}|$, of both pulses is assumed to be much larger than L . This enables one to neglect the group velocity dispersion (GVD) inside the non-linear medium. Therefore, the time co-ordinate may be treated as a parameter.

(e) Each pulse is divided into $4N$ slices, each one having a duration of $\tau_{\text{slice}} = \tau_{\text{HW1-ej}}/N$. The minimum slice number required ($N = 50$) is obtained from both the energy conservation and the reproducibility in the time-integrated picture against increasing N twice. Totally, $4N$ slices are taken into account.

(f) As a consequence of the above-mentioned assumptions, the initial temporal delay, τ_d , can be involved adequately if $\tau_d = M \tau_{\text{slice}}$, where M is an integer.

Under these assumptions Equation 1 can be rewritten in the form:

$$i \frac{\partial \psi_p}{\partial z} + \alpha_p \left(\frac{\partial^2}{\partial x^2} + \frac{\partial^2}{\partial y^2} \right) \psi_p + k^{\text{SPM}}(\lambda_p) |\psi_p|^2 \psi_p = 0 \quad (3a)$$

$$i \frac{\partial \psi_s}{\partial z} + \alpha_s \left(\frac{\partial^2}{\partial x^2} + \frac{\partial^2}{\partial y^2} \right) \psi_s + k^{\text{IPM}}(\lambda_s) |\psi_p|^2 \psi_s = 0 \quad (3b)$$

where ψ_p and ψ_s denote the slice amplitudes of the pump and probe. The beams-pulses are assumed to be described by:

$$\psi_p(r, z=0, t) = A_p \exp\left(-\frac{r^2}{a_p^2}\right) \exp\left(-\frac{t^2}{2\tau_p^2}\right) \quad (4a)$$

$$\psi_s(r, z=0, t) = A_s \exp\left(-\frac{r^2}{a_s^2}\right) \exp\left[-\frac{(t-\tau_d)^2}{2\tau_s^2}\right] \quad (4b)$$

and the spatio-temporal co-ordinate system is taken to be connected to the pump. In Equations 4, a_p and a_s are the beam radii at the focusing lens, τ_p and τ_s are the pulse durations, τ_d is the temporal delay between pulses and t is the slice local time ($t=0$ corresponds to the temporal maximum of the pump pulse). The energy transmitted through the aperture is estimated after integration over the probe slices, i.e. on the time profile of the probe pulse, with a subsequent integration over the aperture cross-section. Normalized transmittance is defined as a ratio of the probe beam-pulse transmittance to the probe transmittance in the absence of a pump. In the numerical analyses the authors consider three types of non-linear media: a crystal with a fast electronic non-linearity, a liquid with a reorientational Kerr non-linearity and, finally, a resonant noble gas medium. The response time of the solid-state crystal material is expected to be of the order of or less than 10^{-14} s. According to the Z-scan measurements of [11], BaF₂ has a relatively high third-order non-linearity [$n_2^{\text{SPM}} = (0.9 \pm 0.15) \times 10^{-13}$ esu at 532 nm and 10^{-13} esu at 1.06 μm]. Its transparency region spans from 250 nm to 9 μm . The dispersion of n_2 is expected to be negligible in this region. Although many semiconductor-based materials have higher non-linear coefficients, their short-wavelength cut-off is limited to the infrared and near-infrared region. In Fig. 2 the normalized transmittance versus normalized delay ($|\tau_d|/\tau_p$) for a non-resonant medium (BaF₂) is shown. In this case the self-action of the pump wave is taken into account. The model parameters are $\lambda_p = 1.064 \mu\text{m}$, $\lambda_s = 532 \text{ nm}$, $f = 10 \text{ cm}$, $L = 2.4 \text{ mm}$, $n_2^{\text{SPM}} = n_2^{\text{IPM}} = 0.9 \times 10^{-13}$ esu [11]. The pump intensity is chosen to be 100 GW cm^{-2} in the linear beam waist. The radii of the pump and probe beams at the lens are 1.125 and 0.56 mm, respectively; where $z_0 = 0.531 \text{ cm}$, the lens-to-aperture distance equals 60 cm and the non-linear medium is placed at $z = 0.86z_0$. The thickness of the non-linear medium, L , and the aperture size, S , are chosen according to the condition for a well-expressed contrast in the aperture transmittance [11] [$L \ll z_0$, $S = 1 - \exp(-2r_a^2/w_a^2) = 0.01$ at an aperture radius $r_a = 100 \mu\text{m}$, w_a being the beam radius at the aperture in the linear propagation regime]. In Fig. 2 the dots indicate the numerical results for different values of $|\tau_d|/\tau_p$. The solid lines are the Gaussian approximations, of the form:

$$T^{\text{Gaus}} \propto \exp\left(-\frac{\tau_d^2}{\tau_s^2 + \tau_p^2}\right) \quad (5)$$

where T is the normalized transmission of the aperture. Curves (a-c) on Fig. 2 correspond to $\tau_s = (1/3)\tau_p$, $\tau_s = \tau_p$, $\tau_s = 3\tau_p$, respectively.

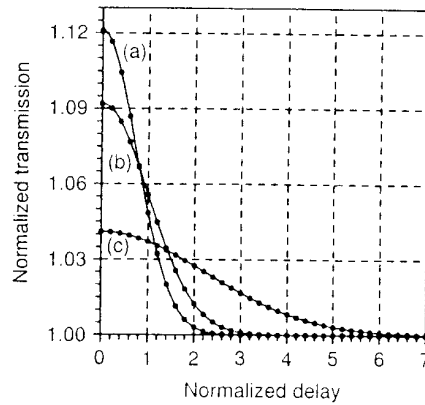


Figure 2 Normalized aperture transmission as a function of the normalized delay, $|\tau_d|/\tau_p$, for $\tau_s/\tau_p = 1/3$ (curve a), 1 (curve b), and 3 (curve c). Non-linear medium, BaF₂. The model parameters are $\lambda_p = 1.064 \mu\text{m}$, $\lambda_s = 532 \text{ nm}$, $f = 10 \text{ cm}$, $L = 2.4 \text{ mm}$, $n_2^{\text{SPM}} = 0.9 \times 10^{-13} \text{ esu}$; and intensity in the linear beam waist, 100 GW cm^{-2} .

CS₂ and nitrobenzene belong to the most popular Kerr non-linear media. The authors' numerical calculations have shown that their large non-resonant third-order susceptibilities allow, in principle, qualitatively and quantitatively the same results to be obtained at lower pump intensities. However, the non-linear response times of CS₂ and nitrobenzene are estimated to be of the order of 2 and 5 ps, respectively [11].

The inert gases are promising non-linear media in the short-wavelength region (u.v. and v.u.v.) [19, 20]. The non-linear susceptibilities for self-phase and cross-phase modulation have a resonant character and response times of the order of 10^{-14} s or less. If the pump and probe wavelengths, λ_p and λ_s , are chosen in the vicinity of $\omega_p + \omega_s$ two-photon resonance, ω_p and ω_s , being far from single- and two-photon resonances, the IPM (XPM) can strongly dominate the SPM [$n_2^{\text{IPM}} \gg n_2^{\text{SPM}}(\lambda_{s,p})$] [21]. Figure 3 plots the results on the T-scanner normalized transmission versus normalized delay, $|\tau_d|/\tau_p$, for gaseous Xe under a pressure of $1.013 \times 10^5 \text{ Pa}$. The authors used the following model parameters: $k^{\text{IPM}} = 8.1 \text{ cm}^2 \text{ erg}^{-1}$ (CGS units); $\lambda_s = 264.42 \text{ nm}$; $\lambda_p = 248 \text{ nm}$; lens focal length, $f = 10 \text{ cm}$; $L = 3 \text{ mm}$; and aperture diameter, $2r_a = 140 \mu\text{m}$. The relatively high value of k^{IPM} is due to the choice of $\omega_p + \omega_s$ near a two-photon resonance at a negligible beam-pulse self-action. The pump intensity in the linear beam waist is chosen to be 10^6 W cm^{-2} . The radii of the pump and the signal beams at the lens are 0.3 and 0.28 mm, respectively. Under these conditions $z_0 = 1.05 \text{ cm}$, the distance between the lens and the centre of the non-linear medium equals 10.75 cm, i.e. $z = 0.86z_0$; whereas the lens-to-aperture distance is 60 cm. The dots in Fig. 3 indicate the numerical results obtained by solving Equations 3, whereas the solid lines are Gaussian fits (Equation 5) with τ_s/τ_p as a parameter.

Qualitatively, the dependence of the normalized transmittance as a function of the initial delay, $|\tau_d|/\tau_p$, is similar under both resonant and non-resonant conditions. Quantitatively, the self-focusing of the pump beam causes an increase of the probe-beam induced focusing, leading to an enhancement of the aperture transmittance. Naturally, the curve's behaviour can reverse if a non-linear medium is placed between the lens and the linear beam waist ($z < 0$) or at negative non-linear refractive index corrections.

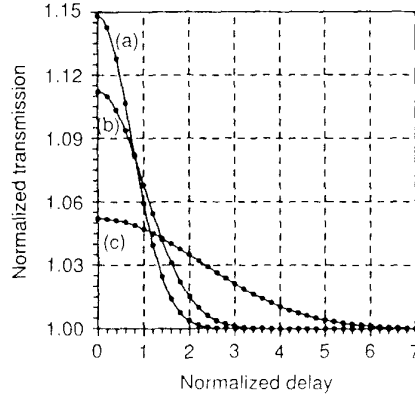


Figure 3 Normalized aperture transmission as a function of the normalized delay, $|\tau_d|/\tau_p$, for $\tau_s/\tau_p = 1/3$ (curve a), 1 (curve b), and 3 (curve c). Non-linear medium, Xe (pressure 1.013×10^5 Pa, $p = 1$). The model parameters are $\lambda_p = 248$ nm, $\lambda_s = 264.42$ nm, $f = 10$ cm, $L = 3$ mm, $n_2^{\text{SPM}} = 2.7 \times 10^{-11}$ esu; and intensity in the linear beam waist, 10^9 W cm $^{-2}$.

3. Variational analysis of the T-scanner

Using the variational approach [22] for solving Equation 1 one obtains results which can motivate the Gaussian dependence of normalized transmittance versus normalized temporal delay, $(|\tau_d|/\tau_p)$. As stated previously, the beam-pulse evolution inside the scanner is described by Equation 1. These equations, in a pump-probe approximation, can be formulated as a variational problem, which corresponds to a Lagrangian of density:

$$L = L_s + L_p + N_s + N_p \quad (6a)$$

where

$$L_j = \frac{i}{2} r \left(v_j \frac{\partial v_j^*}{\partial z} - v_j^* \frac{\partial v_j}{\partial z} \right) + \frac{i}{2} \frac{r}{V_g} \left(v_j \frac{\partial v_j^*}{\partial t} - v_j^* \frac{\partial v_j}{\partial t} \right) + \frac{3}{2} r \left| \frac{\partial v_j}{\partial t} \right|^2 + \alpha_j r \left| \frac{\partial v_j}{\partial r} \right|^2 \quad (6b)$$

$N_p = -k^{\text{IPM}} r |v_p|^2 |v_s|^2$ and $N_s = -(k^{\text{SPM}}/2) r |v_p|^4$ for the probe and pump wave, respectively, and r denotes radial co-ordinate [$r = (x^2 + y^2)^{1/2}$]. In this formulation the problem can be expressed mathematically as:

$$\delta \int L_G dz dr dt = 0 \quad (7)$$

where L_G denotes Lagrangian L after the substitution of the trial functions. The latter ones are assumed to be Gaussian both in time and space (in local times $t' = t - z/V_{g_s}$, $t'' = t - z/V_{g_p}$):

$$v_s(r, z, t') = \frac{A_0(z)}{w_s^2(z)} \exp \left[-\frac{t'^2}{2\tau_s^2} + i b_s(z) t'^2 \right] \exp \left[-\frac{r^2}{a_s^2 w_s^2(z)} - i \frac{k_s \rho_s(z) r^2}{2} \right] \quad (8a)$$

$$v_p(r, z, t'') = \frac{A_p(z)}{w_p^2(z)} \exp \left[-\frac{t''^2}{2\tau_p^2} + i b_p(z) t''^2 \right] \exp \left[-\frac{r^2}{a_p^2 w_p^2(z)} - i \frac{k_p \rho_p(z) r^2}{2} \right] \quad (8b)$$

In Equations 8 $b_{s,p}$ is the pulse chirp, $r_{s,p}$ is the inverse of the radii of curvature of the corresponding wavefront, and $w_{s,p}$ is the normalized beam radii [$w_{s,p} = a_{s,p}(z)/a_{s,p}(z=0)$] for the probe and pump, respectively. Following the variational procedure [22], one obtains a set of ordinary differential equations for the variational parameters $r_{s,p}$, $b_{s,p}$, $w_{s,p}$ and $t_{s,p}$. In order to avoid redundant analytical considerations [23] the authors present the most important results only. It is found that the dependence of the effective non-linearity, $k_{\text{eff}}^{\text{IPM}}$, on the temporal delay, τ_d , has the form:

$$k_{\text{eff}}^{\text{IPM}} = k^{\text{IPM}}(\lambda_s) \exp \left[-\frac{(t_d - z v_{s,p})^2}{\tau_s^2 + \tau_p^2} \right] \quad (9)$$

If one neglects the group-velocity mismatch, Equation 9 takes the form of the Gaussian function (Equation 5) used for fitting the numerically obtained data (see Figs 2 and 3). This result does not seem surprising. In the time-delay scheme analysed, the aperture transmittance can be regarded as the cross-correlation of the pump and probe pulses (provided that the non-linearity response time is instantaneous). From a separate analysis of the T-scan configuration (Fig. 1) based on a matrix-optics approach, one obtains a linear relation between the aperture transmittance and $k_{\text{eff}}^{\text{IPM}}$.

Since $\partial k_{\text{eff}}^{\text{IPM}} / \partial q < 0$, where $q = \tau_d / \tau_p$, the changing rate of transmittance versus τ_d has a maximum when $\partial^2 k_{\text{eff}}^{\text{IPM}} / \partial q^2 = 0$, or:

$$\tau_p^2 = 2\tau_{d,\text{max}}^2 - \tau_s^2 \quad (10)$$

This result agrees exactly with the numerical data shown in Figs 2 and 3 and is proved in the experiment described in the next section.

According to the results presented, the experimental approach for measuring pulse widths using a time-delayed Z-scan configuration (T-scan) should be the following one. It is necessary to obtain the experimental dependence of the normalized transmittance, T , on the temporal delay, τ_d . Differentiating twice the experimental curve, one can obtain the delay, $\tau_{d,\text{max}}$, at which the changing rate of the aperture transmittance, T , has a maximum (as an absolute value). Thereafter, using Equation 10, it is easy to obtain the unknown pulse duration. A restriction of the method is that one of the pulse durations should be known, if the pump and probe pulse widths are different. Unfortunately, for sech^2 pulses, one cannot obtain an analytical result in closed form, as is done for Gaussian pulses. The numerical simulations show that the delay, $\tau_{d(1/e)}$, at which the normalized aperture transmission, $T(\tau_d = 0)$, decreases e-times is related to the widths, τ_s and τ_p , of the sech^2 pulses as:

$$\tau_{d(1/e)} = 0.836(\tau_s + \tau_p) \quad (11)$$

This numerical approximation is found to ensure a relative inaccuracy of less than 5% in the range $\tau_s / \tau_p \in [0.2, 4]$. If the T-scanner is used as an autocorrelator ($\tau_s = \tau_p = \tau$), pump and probe beam-pulse could be of crossed polarizations and the filter in front of the detector should be replaced, for example, by a Glan-prism. The non-linear medium should possess a reorientational Kerr-type non-linearity and, therefore, for which $\text{sign}(n_2^{\text{SPM}}) = -\text{sign}(n_2^{\text{IPM}})$ [13].

4. Experimental results

The experimental set-up used in the T-scan measurement is depicted in Fig. 4. The output pulses from a mode-locked Nd:YAL laser ($\lambda_L = 1.079 \mu\text{m}$) are frequency-doubled in a KDP non-linear crystal [first type of synchronism; conversion efficiency, 5–7%]. The

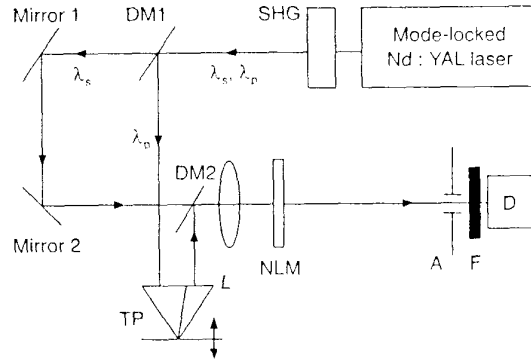


Figure 4 Experimental set-up used for performing a T-scan measurement (see Fig. 1 and text for details). SHG, a nonlinear crystal for second harmonic generation.

second-harmonic pulses, at a wavelength $\lambda_s = \lambda_L/2$, served as probe pulses; whereas the pulses at the fundamental wavelength, $\lambda_p = \lambda_L$, are used as pump pulses. As a result of independent measurement by an AGAT-SF streak-camera (resolution better than 4.5 ps; photofilm, Kodak T_{\max} 400) the duration of the laser pulses is estimated to be $\tau_p^{\text{SC}} = 285$ ps. The dichroic mirrors (DM1 and DM2) and the corner-cube reflector (TP) form a variable delay-line for the pump pulses [$\max(\tau_d) = 2$ ns]. Both beams are adjusted to overlap at the dichroic mirror DM2 and are focused with an achromatic lens ($f = 7.5$ cm). The non-linear medium (NLM) used is nitrobenzene, filled in a 5 mm thick quartz quivette. The response time of the reorientational Kerr effect in this medium, $\tau_{\text{resp}} \approx 5$ ps, is much shorter than the duration of the pulses used and, therefore, can be regarded as instantaneous. The latter is confirmed during the experiments. The aperture (diaphragm with a diameter of $500 \mu\text{m}$) was placed at a distance $L = 50$ cm (see Fig. 1) from the linear focus of the lens. An interference filter (F) was placed behind the aperture to block out the emission at the fundamental wavelength. The energy transmitted was measured with an energy/power meter Laser Precision RJ 7200 and was normalized to the energy transmitted in the absence of a quivette.

In an independent comparative measurement the quivette was replaced by a 3 cm long non-linear KDP crystal for generating the third harmonic of the laser wavelength in a second-type non-linear process, i.e. $\lambda_{\text{TH}} = (1/\lambda_s + 1/\lambda_p)^{-1}$. The entrance face of the crystal was located approximately at the position of the quivette input face in the T-scan configuration. The aperture was removed and a narrow bandpass filter was used to transmit the third harmonic only. Since the signals measured by both methods depend on τ_d (see Equation 9), this is an appropriate approach for verifying the experimental results from the T-scanner.

The result from the T-scan measurement is shown in Fig. 5. The dots indicate the experimental values of the normalized aperture transmittance versus pump pulse delay, whereas the solid curve is a Gaussian fit of the form given by Equation 5. As a result, following the procedure from the previous section, one deduces the duration of the pump pulses, $\tau_p^{\text{T-scan}} = 308$ ps half-width at half maximum (HWHM). The measurement of the third-harmonic signal versus τ_d (see Fig. 6) yields a correlation width of 311 ps, which corresponds (at the Gaussian pulse shape assumed) to a pump pulse duration of $\tau_p^{\text{TH}} = 254$ ps HWHM. The relative difference between the experimental values retrieved is $(\tau_p^{\text{T-scan}} - \tau_p^{\text{TH}}) / (|\tau_p^{\text{T-scan}} + \tau_p^{\text{TH}}|/2) \approx 19\%$, and seems relatively large as compared to the relative difference

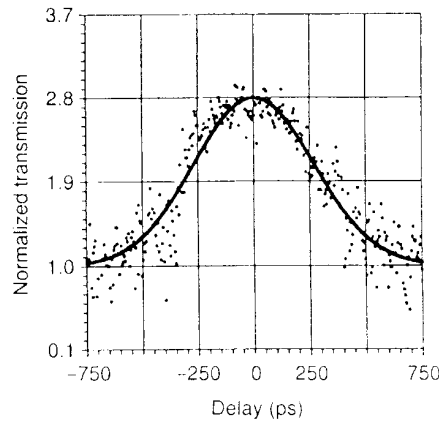


Figure 5 T-scan measurement: normalized aperture transmission versus pump pulse delay.

$(\tau_p^{\text{T-scan}} - \tau_p^{\text{SC}})/(|\tau_p^{\text{T-scan}} + \tau_p^{\text{SC}}|/2) \approx 8\%$ obtained in the streak-camera measurement. The relative inaccuracy of the method analysed and the possible approaches to minimize it will be discussed in the next section.

A significant source of experimental inaccuracy in the measurement arises from the difficulty in controlling the spatial overlapping of the focused first- and second-harmonic beams within the 3 cm long non-linear crystal over the 30 cm long (single pass) delay line used. This problem should be considerably easier to solve at pulses of durations of units of picoseconds or less. It is worth noting that (similar to the second-order correlation functions), the ratio of the third-order correlation width to the pulse-width does depend on the pulse shape assumed, e.g. 0.81 for Gaussian pulses and 0.667 for sech-shaped pulses. Generally, if an independent streak-camera measurement is absent, the assumption of a certain pulse shape leads to an uncertainty of the order of 8%. In view of the above, quantitative agreement of the experimental results could be evaluated at least as satisfactory.

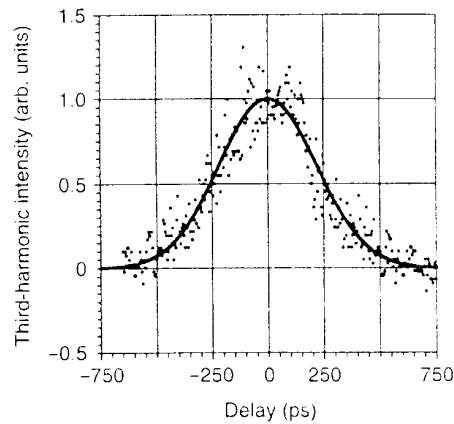


Figure 6 Comparative measurement: third-harmonic intensity versus pump pulse delay.

5. Discussion

The researchers would be motivated to exploit the T-scanner if only it is compatible to the streak-cameras and the autocorrelators currently in use. This technique could appear potentially advantageous in u.v. and v.u.v. spectral ranges, for which transparent non-linear crystals do not exist presently. Optical damage of non-linear media in a liquid and gas phase is reversible, in contrast to that in non-linear crystals. The T-scanner also avoids the necessity of the waves involved to be phase-matched. For measuring femtosecond pulse widths, a non-linear medium with non-linear electronic polarizability should be used (typical response time from 10^{-14} to 10^{-15} s and $n_2^{\text{SPM}} \cong 10^{-8}$ to 10^{-14} esu [24]). At a negligible birefringence the main inaccuracy of the scheme analysed will arise from pulse broadening due to group-velocity dispersion.

The estimations for BaF₂ show that the group-velocity dispersion (GVD) coefficient, β_2 , equals 1.8×10^2 , 2.4×10^2 and 4×10^2 fs² m⁻¹ at 532 and 620 nm and 1.06 μ m, respectively. The authors assume that more than 2% pulse broadening due to GVD inside the non-linear medium can affect drastically the performance of the T-scanner. This is in accordance with the simplifications in the numerical procedure used for solving Equation 1. Therefore, the minimum pulse widths, which could be measured accurately, are 16, 19 and 24 fs at 532 and 620 nm and 1.06 μ m, respectively. Using the T-scanner as an autocorrelator, the relative accuracy of measurement is estimated using:

$$\frac{\Delta\tau}{\tau} = 2 \frac{\Delta\tau_d}{\tau_d} + \frac{\Delta\tau'}{\tau} + \frac{1}{(T-1)} \frac{\Delta T}{T} \quad (12)$$

where $\Delta\tau'$ accounts for the pulse broadening due to GVD inside the non-linear medium.

Considering the experimental geometry in [11], $T_{\text{max}} = 1.1$ and $\Delta T/T = 1\%$, and it is reasonable to assume that $\Delta\tau_d/\tau_d = 3\%$ and $\Delta\tau'/\tau = 2\%$. Therefore, the total accuracy of the measurement seems to be within 20%. The relative error of the measurement with the T-scanner can be reduced at higher contrast in the aperture transmissions, T versus τ_d .

To estimate the accuracy of the method at different pump and probe pulse durations, the authors use the notation $t_s = p t_p$ and Equation 5. Under the condition $|T-1| \ll 1$, the relative error of p is:

$$\frac{\Delta p}{p} = \left(1 + \frac{1}{p^2}\right) \left[\frac{\Delta\tau_d}{\tau_d} + \frac{\Delta\tau_p}{\tau_p} + \frac{1}{2(T-1)} \frac{\Delta T}{T} \right] \quad (13)$$

From the experimental data presented in Section 4, the total inaccuracy was evaluated to be within 20%.

The non-linearity in the walls of the vessel containing the non-linear medium could appear non-negligible, but it should affect the amplitude of the aperture transmittance, not its behaviour versus τ_d . If chirped pulses are measured with the T-scanner, their duration should be corrected for their GVD broadening along the propagation path from the exit of the laser to the exit face of the quivette (e.g. for GVD in air: from the laser source to the entrance face of the lens and from their output face to the quivette; for GVD in quartz: inside the lens and the quivette entrance window; and for GVD in the non-linear medium). The delay line will broaden additionally the probe pulse. Similar problems, however, arise when other methods, e.g. autocorrelation techniques, are used.

In the numerical model the authors neglect the group-velocity mismatch, which is estimated to be $v_{s,p} = 1.8 \times 10^{-2}$ ps cm⁻¹ for Xe ($\lambda_s = 264.42$ nm, $\lambda_p = 248$ nm), and 0.57 ps cm⁻¹ for CS₂ ($\lambda_p = 1.06$ μ m, $\lambda_s = 532$ nm). With the parameters considered, accounting for the

restrictions of the simplified numerical procedure used, pulse durations down to 1 ps with Xe and 6 ps with CS₂ can be measured. Actually, a more serious restriction for CS₂ is posed by the non-linear response time of CS₂ (2 ps) [4, 11]. The noble gases may appear practical for use in the short wavelength spectral range where transparent condensed non-linear media are not available.

6. Conclusions

The authors have shown that the induced phase modulation in a T-scan geometry can be used for measuring ultrashort pulses. Both numerical and variational approaches reveal that a simple and practical device seems feasible. Quantitative agreement between the experimental results of a T-scan measurement, time-delayed third-harmonic generation and independent streak-camera measurement supports this statement. In the case of a BaF₂ crystal the electronic non-linearity allows, in principle, pulses as short as 20 fs to be measured. In the case of Xe and CS₂ the shortest pulse duration, which can be accounted for by the simplified numerical model, is of the order of units of picoseconds.

7. Acknowledgements

The authors would like to acknowledge the contribution of D. Kavaldjiev. This work was done with the financial support of the National Science Foundation, Bulgaria.

References

1. K. MÖLLMANN, W. GELLERMANN and H. WELLING, in *XVIII International Quantum Electronics Conference IQEC'92*, 14–19 June 1992, Vienna, Austria (Tech. Univ. Wien, Vienna, Austria, 1992) paper MoD4.
2. M. T. ASAKI, C.-P. HUANG, D. CARVEY, J. ZHOU, H. C. KAPTEYN and M. MURNANE, *Opt. Lett.* **18** (1993) 977.
3. C. EDELSTEIN, E. WACHMAN, L. K. CHENG, W. R. BOSENBĚRO and C. L. TANG, *Appl. Phys. Lett.* **52** (1988) 2211.
4. S. L. SHAPIRO, *Topics in Applied Physics: Ultrafast Light Pulses, Picosecond Techniques and Applications* (Springer-Verlag, Berlin, 1977) pp. 18–36.
5. W. MÜCKENHEIM, P. LOKAL, B. BURGHARDT and D. BASTIG, *Appl. Phys. B* **45** (1988) 259.
6. A. TÖNNERMANN, H. EICHMANN, R. HENKING, K. MOSSAVI and B. WELLEGHAUSEN, *Opt. Lett.* **16** (1991) 402.
7. P. B. CORKUM and V. D. TARANUKHIN, in *Technical Digest, 15th International Conference on Coherent and Nonlinear Optics, ICNO'95*, 27 June–1 July 1995, St Petersburg, Russia and Vol. 1 (Optical Society, St. Petersburg, Russia, 1995) p. 125.
8. J. I. DAGAP, G. B. FOCHT, D. H. REITZE and M. C. DOWNER, *Opt. Lett.* **16** (1991) 499.
9. I. BUCHVAROV, S. SALTIEL, V. GUSEV and V. PLATONENKO, *J. Phys. D* **22** (1989) 1423.
10. H. NISHIOKA, M. ISHIGURO, T. KAWASUMI, K. UEDA and H. TAKUMA, *Opt. Lett.* **18** (1993) 45.
11. M. SHEIK-BAHAE, A. A. SAID, T. WEL, D. HAGAN and E. W. VAN STRYLAND, *IEEE J. Quant. Electron.* **QE-26** (1990) 760.
12. H. MA, A. S. L. GOMES and C. B. DE ARAUJO, *Appl. Phys. Lett.* **59** (1991) 2666.
13. M. SHEIK-BAHAE, J. WANG, R. DESALVO, D. J. HAGAN and E. W. VAN STRYLAND, *Opt. Lett.* **17** (1992) 258.
14. M. SHEIK-BAHAE, J. R. DESALVO, J. W. WANG, D. J. HAGAN and E. W. VAN STRYLAND in *CLEO'91 Digest*, 12–17 May 1991, Baltimore MD, USA (Opt. Soc. of Am., Washington DC, 1991), paper CTuW16, p. 180.
15. J. WANG, M. SHEIK-BAHAE, A. A. SAID, D. J. HAGAN and E. W. VAN STRYLAND, *CLEO'92 Digest*, 10–15 May 1992, Anaheim, CA, USA (Opt. Soc. of Am., Washington DC, 1992) paper CTu16, p. 450.
16. R. R. ALEANO and P. P. HO, *IEEE J. Quantum. Electron.* **QE-24** (1988) 351.
17. M. LISAK, A. HÖÖK and D. ANDERSON, *J. Opt. Soc. Am. B* **7** (1990) 810.
18. Y. SILBERBERG, *Opt. Lett.* **15** (1990) 1282.
19. A. H. KUNG, *Opt. Lett.* **8** (1983) 24.
20. H. EGGER, R. T. HAWKINS, J. BOKOR, H. PUMMER, M. ROTHSCILD and C. K. RHODES, *Opt. Lett.* **5** (1980) 282.
21. S. DINEV, A. DREISCHUH, D. KAVALDJEV and K. KRASIEV, *J. Opt. Soc. Am. B* **9** (1992) 387.
22. D. ANDERSON, M. LISAK and T. REICHEL, *Phys. Rev. A* **38** (1988) 1618.
23. S. DINEV, A. DREISCHUH and S. BALUSCHEV, *Physica Scripta* **47** (1993) 792.
24. G. P. AGRAWAL, *Nonlinear Fiber Optics* (Academic Press, London, 1989) p. 42.